https://doi.org/10.5194/hess-2023-240
Preprint. Discussion started: 16 October 2023

Hydrology and Earth System Sciences
Discussions
Open Access

Soil water sources and its implications on vegetation restoration in the Three-river Headwaters Region during different ablation periods

Zongxing Li [1]*, Juan Gui [1], Baijuan Zhang [1]

Key Laboratory of Ecohydrology of Inland River Basin/Gansu Qilian Mountains Eco-Environment Research Center/ Observation and Research Station of Isotope Eco-Hydrology and National Park in Alpine Mountains Region, Northwest Institute of Eco-Environment and Resources, Chinese Academy of Sciences, Lanzhou 730000, China

*Corresponding author: Tel: 86+13919887317, E-mail: lizxhhs@163.com (Zongxing Li).

Abstract: Under climate warming, effective restoration and protection of the ecological environment could happen by timely supplementing soil water. So it is crucial to understand the spatial-temporal changes in soil water sources. Two thousand six hundred samples of soil water, precipitation, river water, ground ice, supra-permafrost water, and glacier snow meltwater have been collected ~~from~~ June, August, and September 2020 to quantify the soil water sources in the Three-River Headwater Region under different ablation periods. Results indicated that precipitation, ground ice, and snow meltwater accounted for approximately 72%, 20%, and 8% of soil water during the early ablation period. Snow is completely melted in the heavy and the end of the ablation period, and precipitation contributed to about 90% and 94% of soil water, respectively. These recharges also vary markedly with altitude and vegetation type. Various factors influence soil water sources, including temperature, precipitation, vegetation, evapotranspiration, and the freeze-thaw cycle. However, soil water loss will further exacerbate vegetation degradation and pose a significant threat to the ecological security of the "Chinese water tower." So there is an urgent need to monitor soil water, warn of vegetation degradation associated with soil moisture loss, and identify reasonable water-soil conservation and vegetation restoration patterns.

Keywords: soil water sources, precipitation, ground ice, three-River Headwater Region

1. Introduction

Soil water is a vital water resource, a link between precipitation, surface water, soil water, and groundwater, which is an essential component in the formation, transformation, and consumption of water resources with spatial-temporal scales. It substantially impacts regional water resource distribution patterns, the ecological environment, and river runoff as the key factors in terrestrial hydrological cycles and environmental succession (Gao et al., 2017; Sazibet al., 2020). Soil water plays a fundamental role in controlling the exchange of water and heat between the land surface and atmosphere, which has been widely applied to study the regional microclimate, energy and material balance, and global climate change (Spennemann et al., 2017; Sprenger, Tetzlaff, & Soulsby, 2017). Moreover, soil water is directly involved in physiological activities and promotes productivity and carbon sequestration capacity. It was sensitive to the interaction between soil and vegetation that altered soil physicochemical properties, internal structures, and material composition (Marchionni et al., 2021). Consequently, soil water sources can be affected by many factors, such as climate, vegetation, soil type, and topography (Martinez Garcia et al., 2014). Understanding the spatial-temporal changes in soil water sources is essential for better projection of the water and ecology. So, studying soil water sources is a hot topic in international hydrology and soil science.

Research on soil water has progressed in a series of studies related to the hydrometeorological, hydro-climatological, ecological, and biogeochemical processes. Permafrost existence can affect inter-annual changes in soil water, and its degradation, including the increasing active layer thickness and disappearance, would decrease ecosystem resilience (Liu et al., 2021). At high latitudes, active-layer deepening associated with soil water changes occurred over less than 8% of the current permafrost area under climate warming (Zachary et al., 2013). Soil water modulates regional climate from sub-seasonal to seasonal timescales. Zhang et al.

(2020) found that drier soil led to a more significant increase in the upper quantile of summer heatwaves frequency than in the lower quantile. Liu et al. (2014) thought wet (dry) initial soil water anomalies reduce (amplify) the drought extremes, diminish (reinforce) the hot extremes, and enhance (reduce) the cold extremes over areas of strong soil water-atmosphere coupling. Qi et al. (2020) found that soil water could decrease by at least 20% in March-May if there is no snow. Alexander (2021) also found that despite the high humidity in autumn and the high snow reserves accumulated during winter, soil water decreased after the snow had melted. The soil water movement is an important carrier of the material cycle and energy flow. The horizontal flow weakens in the freezing period due to the terrain slope and the freezing-thawing cycle, whereas the vertical migration of soil water moves and strengthens (Cao et al., 2017). Zhang et al. (2021) investigated the water movement in reconstructed soil and evaluated the effects of mining waste rock on plant growth in an arid-cold region. The interaction between soil water and the ground thaw was more dependent at wetter sites, and the interactive soil water and thaw depth behavior on hill slopes changed with location (Guan et al., 2010). Inter-annual anomalies of soil water and vegetation due to rainfall during a given summer were maintained through the freezing winter to the spring, acting as an initial condition for subsequent summer land-surface and rainfall conditions (Masato and Banzragch, 2011). Based on the observation in the central

https://doi.org/10.5194/hess-2023-240
Preprint. Discussion started: 16 October 2023

Tibetan Plateau, the four GLDAS models tend to systematically underestimate the surface soil water (0-5 cm) while well simulated the soil water for the 20-40 cm layer, especially during the soil thawing period (Chen et al., 2013; Li et al., 2019). The vegetation effect and the freezing-thawing cycle may be the significant factors that led to an unsatisfactory performance of the Soil Moisture Active Passive (SMAP) mission (Wagner et al., 2003; Ma et al., 2017). As mentioned above, the quantification of soil water sources is relatively insufficient.

Soil water has also been deeply concerned in TRHR. Cao and Jin (2021) analyzed the distribution characteristics of soil water and its relationship with temperature and precipitation in TRHR. The influence of precipitation on soil water in the alpine steppe was greater than that in an alpine meadow, especially in lower-altitude areas (Li et al., 2022). Chen et al. (2021) constructed the spatial-temporal changes in soil water and its influencing factors from 2003 to 2020. Huang et al. (2022) studied the variation of surface soil water in an alpine meadow with different degradation degrees in the study region. Xing et al. (2016) analyzed the groundwater storage changes and their influence on soil water in the TRHR. Guo et al. (2022) thought the main factors influencing soil water changes were NDVI and precipitation, followed by air temperature and wind speed in the sources region of the Yellow river. Land degradation significantly reduced soil water by 4.5-6.1% at a depth of 0-100 cm and increased the

https://doi.org/10.5194/hess-2023-240
Preprint. Discussion started: 16 October 2023

annual mean soil surface temperature by 0.8 °C under climate warming in the sources region of the Yangtze river (Xue et al., 2017). Soil water and temperature showed decreasing trends from 0-80 cm and an increasing trend from 80-100 cm (Li et al.,2020). The change of soil water resulted in vegetation degeneration, soil desertification, and leanness in the source regions of the Yangtze River (Wang et al., 2012), and it also had a positive correlation with the average thickness of wind deposition (Song et al., 2019). The TRHR is undergoing a glacier retreat, permafrost degradation, precipitation increase, snowfall decrease, water conservation decrease, and soil erosion intensification under climate warming (Li et al., 2021). These changes have caused large fluctuations of soil water, bringing great uncertainty to vegetation growth and causing challenges in vegetation restoration. So there is an urgent need to quantify the soil water sources to improve the effectiveness of ecological restoration in permafrost regions.

However, the field observations are too sparse to satisfy the need for quantifying soil water sources in TRHR. As the natural tracers, stable isotopes can be applied in water cycle studies to trace precipitation, soil water, groundwater, and plant water (Zhang et al., 2017; Wang et al., 2018; Yang et al., 2019; Li et al., 2022). Monitoring the stable isotope characteristics of soil water could provide information about water sources, changes in soil water, and moisture cycling (Sprenger et al., 2017). So based on 2600 samples of soil water, precipitation, river water, ground ice,

https://doi.org/10.5194/hess-2023-240
Preprint. Discussion started: 16 October 2023

supra-permafrost water, and glacier snow meltwater collected from June, August, and September 2020, this study (a) analyzes the spatiotemporal distribution of δ^2H and δ^{18}O in soil water at different ablation stages; (b) discusses the hydrological processes of soil water and its differences; (c) quantifies the major sources and its contributions to soil water; (d) confirms the corresponding implications for ecological protection. The result presents new observational evidence of soil water sources in the "Chinese Water Tower." It provides a scientific basis for establishing a complex interplay between soil water and vegetation as a theoretical basis for developing water-soil conservation and vegetation restoration patterns in cold regions, especially in the permafrost region.

2. Data and methods

2.1 Study region

Three-River Headwater Region (TRHR) (31°39′-36°12′N, 89°45′-102°23′E, 2610-6920m a.s.l.) is the source region of Yangtze (YZR), Yellow (YLR), and Lancangjiang Rivers (LCR), which is significant to freshwater resources in China and Asia (Fig.1). The TRHR is $36.3T10^4$ km^2 and accounts approximately 50.4% of the total area of the Qinghai Province. The region has a plateau continental climate with an annual average temperature of -5.38-4.14℃ and annual precipitation of 262.2-772.8 mm (Cao and Pan, 2014). The radiation is abundant, with total annual sunlight as high as 2300-2900 h due to the high altitude. The permafrost is extensively developed and is well distributed in the YZR with a depth averaging between 50 and 120 m, whereas permafrost was discontinuous and sporadic with a depth below 50 m in the YLR and LCR (Zhang et al., 2001b). The YLR, YZR, and LCR cover 167,000 km^2, 159,000 km^2, and 37,000 km^2, accounting for 46%, 44%, and 10% of the total area of TRHR, respectively. The YLR, YZR, and LCR contribute approximately 49%, 25%, and 15% of the total runoff and supply up to 600 $\times 10^8$ m^3/a freshwater resources. Additionally, more than 180 rivers, 1800 lakes, 2000 $\times 10^8$ m^3 of glaciers, and 73,300 km^2 of wetlands are present in the TRHR. Protecting the ecology of the TRHR, maintaining and improving its function of water-soil conservation, and water containment are of vital importance to the stable supply of water resources, as well as to climate stability, ecological security, and sustainable economic and social development in Asia. The first largest national park, the Three-River Headwaters National Park, has been built, a restorative practice region for constructing ecological civilization and beautifying China.

Grasslands are the main ecosystems and comprise approximately 70% of the regional vegetation area. The grasses are typical for alpine meadows and alpine steppes, dominated by *Kobresia capillifolia, Kobresia humilis, Stipa purpurea, Elymus dahuricus,* etc. Other vegetation types are temperate steppe and alpine desert with small distributions, dominated by

https://doi.org/10.5194/hess-2023-240
Preprint. Discussion started: 16 October 2023

Hydrology and Earth System Sciences
Discussions

Stipa spp., Achnatherum splendens, Carex spp., and Thylacospermum caespitosum, Androsace tapete, Oxytropis sp., Saussurea subulata, respectively (Fan et al., 2010). Moreover, the ecosystems in the TRHR are characterized by diversity, fragility, sensitivity, weak carrying capacity, and restoration capacity. Most of the soils are thin in thickness and coarse in texture. From high altitude to low altitude, the soil types are alpine desert soil, alpine meadow soil, alpine steppe soil, mountain meadow soil, grey-cinnamon soil, castanozems, and mountain forest soil, respectively. The alpine meadow soil is the primary soil type in the region, and other intrazonal soils are also commonly developed.

2. 2 Data and methods

2.2.1 Samples: collection and preparation

Primary data was collected through fieldwork in June, August, and September 2020. It was used to explore the seasonal pattern and its influence on soil-water sources. A scientific understanding of vegetation restoration in the "Chinese Water Tower" (Fig.2) was developed from these soil-water sources. A total collection of 2600 samples includes soil water, ground ice, precipitation, river water, supra-permafrost water, and glacier snow meltwater in the ~~Three river Headwaters Region~~, with spatial and temporal frequency (Fig.3). The sampling details are described in the following sections.

Soil samples: The soil profile was excavated, and its thickness can be

https://doi.org/10.5194/hess-2023-240
Preprint. Discussion started: 16 October 2023

Hydrology and Earth System Sciences
Open Access
Discussions

determined based on the actual thickness of the soil layer, and the samples were collected at 20 cm intervals from 79, 70, and 93 sampling sites in June, August, and September, respectively (Fig.3). Meanwhile, soil temperature was measured in ºC, and the test range was from −40 ºC to 100ºC, with a ± 0.5ºC accuracy. Soil moisture was measured as a % (m^3/m^3), with a test range of 0 to 100% and a response time of less than 2s. Three parallel samples were collected from each layer for soil water stable isotope analysis. The samples were collected from 2 cm below the surface to avoid the soil samples being influenced by the free atmosphere. ~~Seven hundred forty-one~~ soil samples were collected and stored in HDPE bottles and sealed with parafilm.

Precipitation samples: At Zhimenda (92.26°E, 34.14°N, 3540 m), Tuotuohe (34.22°N, 92.24°E, 4533 m), Zaduo (32.53°N, 95.17°E, 4066.4 m), Dari (33.45°N, 99.39°E, 3967 m) and Maduo (34.55°N, 98.13°E, 4272.3 m) stations, a total of 375 precipitation event-scale samples were collected during from June 2019 to July 2020 in TRHR (Fig.3). All precipitation occurring from 20:00 on the first day to 20:00 the next day was collected from sampling the precipitation event. During sample collection, precipitation, air temperature, wind speed, and relative humidity were recorded at the corresponding national meteorological stations. In order to avoid evaporation, the sample was collected immediately after the

https://doi.org/10.5194/hess-2023-240
Preprint. Discussion started: 16 October 2023

event.

Ground ice: In order to collect the ground ice samples, a 1m deep soil profile of the active permafrost layer was dug at each of the sampling sites, to look for permafrost ground ice (Fig.3). ~~The~~ 66, 40, and 37 ground ice samples have been obtained on June, August, and September, respectively, in the TRHR, which were preserved in pre-cleaned HDPE bottles sealed with parafilm and kept frozen. The outer layer of each ice sample was chipped off to avoid contamination from the soil.

River water: The river water has also been collected in TRHR, including 259, 231, and 186 samples in June, August, and September, respectively, to analyze the spatial and temporal relationship between soil and river water. River water samples were collected 20 cm below the river surface and stored in HDPE bottles sealed with parafilm.

Supra-permafrost water: Supra-permafrost water is mainly stored in the active permafrost layer (Li et al., 2020). To study the hydraulic connection between supra-permafrost water and soil water, 125, 161 and 130 samples were collected at different altitudes during June, August, and September of 2020, respectively. First, a 1-m deep profile of the active permafrost layer was manually dug at each sampling site. Second, the collected water samples were immediately filtered with a 0.45-μm millipore filtration membrane at the bottom of each profile, and then stored in HDPE bottles and sealed with parafilm.

https://doi.org/10.5194/hess-2023-240
Preprint. Discussion started: 16 October 2023

Glaciers snow meltwater: At Jianggudiru Glacier (91°E,33.45°N, 5281 m), Dongkemadi Glacier (92°E, 33°N, 5423 m), and Yuzhufeng Glacier (94.22°E, 35.63°N, 5180 m) in the sources region of Yangtze river (Fig. 1), and Halong glacier (99.78°E, 34.62°N, 5050 m) in the sources region of Yellow river, and Yangzigou glacier (94.85°E, 33.46°N, 5260 m) in the sources region of Lancangjiang river, 27, 32 and 41 samples were collected from streams flowing out of the glacier front during June, August and September of 2020, respectively, and were then stored in HDPE bottles and sealed with parafilm.

Before analysis, all samples were stored at 4 °C in a refrigerator without evaporation. Soil water had to be extracted from the soil. We used a cryogenic freezing vacuum extraction system (LI-2000, Beijing Liga United Technology Co., Ltd., China) to extract soil water, as it can achieve complete extraction and has a high precision (Li et al., 2016). The test tubes containing soil samples were installed on the extraction line and frozen with liquid nitrogen. After 10 min, the line was checked to ensure no leaks. After it was completely sealed, the larger test tube was heated using a heating sleeve at 95 °C, and the smaller test tube was frozen with liquid nitrogen (-196 °C). Due to temperature gradients, water vapor moved from the larger test tube to the smaller one and condensed into ice. The extraction process took 2 hr and had an efficiency above 98%. Water

https://doi.org/10.5194/hess-2023-240
Preprint. Discussion started: 16 October 2023

samples were analyzed for $\delta^{18}O$ and ^{2}H through laser absorption spectroscopy (liquid water isotope analyzer, Los Gatos Research DEL-100, USA) at the Key Laboratory of Ecohydrology of Inland River Basin, Northwest Institute of Eco-Environment and Resources, CAS. The results are reported relative to the Vienna Standard Mean Ocean Water (VSMOW). Measurement precisions for $\delta^{18}O$ and $\delta^{2}H$ were better than 0.5‰ and 0.2 ‰, respectively.

In addition, air temperature, precipitation, evaporation, and ground temperature in the TRHR were mainly obtained from the China Meteorological Data Network (http://data.cma.cn/). The normalized Vegetation Index (NDVI) is derived from MODIS data, downloaded from the NASA website (https://search.earthdata.nasa.gov/), with a spatial resolution of 0.05° and a temporal resolution of 16d, and the data are in HDF format.

2.2.2 Methods

The end member mixing analysis (EMMA) tracer approach has been widely used for analyzing potential soil water sources (Hooper et al., 1990; Hooper, 2003; Gibson et al., 2005; Peng et al., 2012; Li et al., 2014; 2020). The EMMA tracer method assumes that i) the tracer concentration in a potential water source varies significantly in time and space, ii) the chemical properties of the selected tracer are stable, and iii) changes occur as a result of water mixing. Tracer techniques involve graphical analyses

https://doi.org/10.5194/hess-2023-240
Preprint. Discussion started: 16 October 2023

in which chemical and isotopic parameters represent the designated end members. Essentially, the changing composition of the studied water likely results from the intersections during its passage through each landscape. Tracers can be used to determine the sources and flow paths. Both the two- and three-component methods can be described by a uniform equation:

$$Q_t = \sum_{m=1}^{n} Q_m,\quad Q_t C_t^j = \sum_{m=1}^{n} Q_m C_m^j,\ j = l,\ldots,k \quad (1)$$

where Q_t is the total runoff discharge, Q_m is the discharge of component *m*, and $C^m{}_j$ is the tracer *j* incorporated in the component *m*. In addition, the global meteoric water line (GMWL), local meteoric water lines (LMWLs), and evaporation line (LEL) have been used to analyze the relationship between soil water and other waters in the TRHR.

3. Results

3.1 $\delta^{18}O$ and δ^2H of soil water in different ablation periods

Soil water stable isotopes show significant changes in the early ablation period (June), the substantial ablation period (August), and the end of ablation (September). The average value of $\delta^{18}O$ and δD is relatively higher in June and negative in August. Again it becomes higher in September, while it exhibits an opposite trend for d-excess (Table.1). Two reasons can explain this variation: (1) precipitation gradually increases from June, reaches a maximum in August, and then decreases; (2) the effect of evapotranspiration on soil water also shows seasonal variations. Soil water

https://doi.org/10.5194/hess-2023-240
Preprint. Discussion started: 16 October 2023

stable isotopes in different ablation periods show apparent regional differences. This reflects that precipitation is the main source of soil water, and the differences in precipitation stable isotopes are reflected in that of soil water. The temporal variation of stable isotope in 20–80 cm, similar to the TRHR, is progressively negative in the surface soil (0–20 cm). This is due to its high susceptibility to perturbation, and environmental changes (Table.1). Soil water stable isotopes on the eastern slope were gradually negative from June to September, while the other slope directions were consistent with the TRHR (Table.1). Moreover, the strong ablation period of soil water isotopes in meadow and grassland areas was gradually negative from the beginning to the end of ablation, whiles it was continuously negative in forest areas (Table.1). These facts show the stochastic nature of soil water changes as the indicators of environmental changes.

As Fig. ~~3~~ shows, the slope and intercept for LEL are the lowest in the heavy ablation period ~~and then in~~ the early ablation period and the end ablation period, which reflects the seasonal variation of the influence from evaporation or non-equilibrium dynamic fractionation. In contrast, these values gradually increase from June to September in the TRHR. The slope and intercept of LEL for the 0–40 cm layer were the lowest during the heavy ablation period, whiles they were relatively high at the beginning and end of ablation, whereas the slope and intercept of the 40–80 cm layer

https://doi.org/10.5194/hess-2023-240
Preprint. Discussion started: 16 October 2023

gradually increased (Fig.4). This reflects that the soil layer above 40 cm is greatly disturbed by the environment. Its variation is more sensitive to environmental changes, while the deeper soil layer is relatively stable. For different altitudes, the slope and intercept of LEL increased continuously from the beginning to the end of ablation at 3000–3500 m and 5100 m, while at 3500–4500 m the heavy ablation period ~~was~~ the lowest and the beginning and end of ablation were relatively high (Table.2). In the grassland, forest and scrub areas, the slope and intercept of LEL are higher during the heavy ablation period and lower at the beginning and end of ablation, whiles the opposite is evident in the meadow areas (Table.2). More interestingly, the slope and intercept of LEL on the northern and eastern slopes are lower during the heavy ablation period and higher at the beginning and end of the ablation period; on the southern and western slopes, they gradually increase and reach the maximum at the end of ablation period (Table.2). These changes again reflect the multiplicity and complexity of factors influencing soil water, and suggest that conducting soil water source should be predicated on continuous systematic sampling at the regional scale.

3.2 Relationship between soil water and surface waters in different ablation periods

In the study region, the LMWL was $\delta^2H = 7.89\delta^{18}O + 12.43$ ($R^2 = 0.97$; $N = 375$) based on event-level precipitation. As Fig.5 shows, soil water was

https://doi.org/10.5194/hess-2023-240
Preprint. Discussion started: 16 October 2023

primarily located on the LWML, suggesting that precipitation was the major soil water source, and some soil water plotted below the LWML owing to high evaporation. The $\delta^{18}O$ and $\delta^{2}H$ values varied among precipitation, ground ice, and snow meltwater in the early ablation period. This suggests that in June, as the permafrost and snow melt, ground ice meltwater, snow meltwater, and precipitation combine to recharge soil water, and that snow meltwater recharge is mainly in the area above 4000 m based on sampling during the expedition. In the heavy ablation period, soil water is located on the LWML in August, with some sampling sites below it because of stronger evaporation (Fig.5). At this time of year, the snowpack has melted away, and the ground ice in the active layer is also melting rapidly, with precipitation and ground ice meltwater recharging the soil water. Soil water lies above the LWML, and the high slope reflects the relatively low influence of evaporation in the end ablation period, while the absence of snow meltwater and the ground ice in the soil has also melted in areas below 4000 m, so precipitation dominates the soil water source (Fig.5). These variations reflect seasonal variability in the soil water sources. They suggest that freeze-thaw cycles are a key influence on soil water variability.

Interestingly, soil water, supra-permafrost, and river water show a clustered distribution at all ablation stages in the TRHR, reflecting a close hydraulic connection. Precipitation first recharges soil water due to permafrost distribution, while some soil water transforms into supra-permafrost water. Then some soil and supra-permafrost water recharge the runoff, reflecting the uniqueness of the hydrological process in cold regions. These facts show that various recharge sources with significant seasonal variations influence soil water sources. The relationship between soil water and the LWML varied significantly at different altitudes; the higher the altitude, the lower the left-hand side of LWML above 4000 m in the end ablation period, and vice versa, below 4000 m(Fig.5). Reflecting the variation of soil water sources at different altitudes in the end ablation period, soil water is mainly recharged by precipitation in areas below 4000 m, while it is also recharged by ground ice meltwater which is strongly influenced by evaporation, resulting in a relatively positive soil water stable isotope. In the early ablation period, the order of altitude is close to the LWML, and as follows: from 3500–4000 m, 4000–4500 m, above 4500 m, and below 3500 m, confirming the variability of soil water sources in different altitudes (Fig.5). On the one hand, precipitation in the area below 4500 m is primarily liquid, while above the area it is mostly snow, which is strongly affected by evaporation when the snow melts, resulting in a relatively positive soil water stable isotope and lower recharge to soil water; on the other hand, precipitation in June is relatively low, while the temperature in the lower altitude area rises faster, and evaporation is strong, which leads to a positive soil water stable isotope. In the heavy ablation period, the distance between the LEL of soil water and the LWML is comparable at different altitudes, being slightly closer below 3500 m and slightly further from the 4000–4500 m, reflecting less altitudinal variability in soil water sources at this time of year, with abundant precipitation dominating the soil water sources and intense evaporation becoming an important factor influencing soil water dynamics (Fig.5).

The relationship between soil water and the LWML also varied significantly by vegetation, with grassland being farthest from the LWML, followed by meadows and frosts at the early and end ablation period. In contrast, it is farthest for meadows, followed by grassland and forests in a heavy ablation period (Fig.5). These variations indicate that: (1) forests have relatively little effect on shallow soil water due to the predominant use of groundwater and the lower effect of evapotranspiration under the shade of the trees; (2) under the relatively low precipitation, the low soil water in grassland, combined with the effect of evapotranspiration, results in relatively positive soil water stable isotopes; (3) soil water stable isotopes are positive when the meadow is growing, and evapotranspiration is intense under the abundant precipitation season. Evapotranspiration mainly dominates the influence of vegetation on soil water sources. These changes indicate the stochastic nature of the soil water sources and the multiplicity of influencing factors.

3.3 Soil water sources in different ablation periods

https://doi.org/10.5194/hess-2023-240
Preprint. Discussion started: 16 October 2023

Hydrology and Earth System Sciences Discussions

Based on the EMMA model, there were significant differences in the d-excess and $\delta^{18}O$ concentrations of ground ice, precipitation, snow meltwater, and soil water during different ablation periods (Fig.6). Accordingly, these $\delta^{18}O$ and d-excess data were selected for analysis because they could effectively characterize the sources. There were large spatiotemporal variations in the $\delta^{18}O$ and d-excess concentrations. Soil water was plotted on a triangle spanning the three end members, suggesting that soil water was a mixture of them in the early ablation period (Fig. 6). Therefore, precipitation was considered as the first end member, and ground ice as the second end member, and snow meltwater was considered as the third end member. Whereas soil water was plotted on a straight line spanning the two end members, suggesting that soil water was a mixture of precipitation and ground ice in the heavy and end ablation periods (Fig. 6). ~~The intersection between the LWML and the LEL is considered to be the isotopic value of the initial water body that recharges the soil water.~~ The intersection between the LWML and the LEL is considered to be the isotopic value of the initial water body that recharges the soil water, and the corresponding $\delta^{18}O$ and $\delta^{2}H$ are -17.63‰ and -127.61‰, -18.81‰ and -136.94‰, -23.04‰ and -170.36‰ during the early, heavy and end ablation period in the TRRH, respectively. These values are extremely close to the corresponding mean monthly precipitation values, reflecting

https://doi.org/10.5194/hess-2023-240
Preprint. Discussion started: 16 October 2023

that precipitation is the main source of soil water.

Based on the calculation, precipitation, ground ice, and snow meltwater account for approximately 72%, 20%, and 8% of soil water, respectively (Fig.7). Moreover, the recharge pattern shows a ~~clear difference in altitude~~, with no snow meltwater recharge below 4000 m due to snow melting depletion and a higher snow meltwater recharge at higher elevations. The maximum of ground ice meltwater recharge occurs at 3500–4000 m and decreases with increasing altitude. This reflects that the change in altitude of snow and ground ice meltwater is a key factor affecting the source of soil water during the early ablation period. Regarding different vegetation types, ground ice meltwater is higher in meadow areas. In contrast, snow meltwater recharge is relatively high in grassland areas and mainly in precipitation recharge in forest areas. Ground ice and snow meltwater recharge is significantly higher on shaded slopes than on sunny slopes (Fig.7).

In the heavy ablation period, precipitation and ground ice accounted for approximately 90% and 10% of soil water in the TRHR, respectively. Snow is completely melted at this time of year, and the recharge of soil water by precipitation decreases with increasing altitude, while ground ice meltwater gradually increases, ~~with all below 3500 m being recharged by precipitation~~. The forested area is fully recharged by precipitation, while the meadow area is recharged by ground ice meltwater higher than the

https://doi.org/10.5194/hess-2023-240
Preprint. Discussion started: 16 October 2023

Hydrology and Earth System Sciences
Open Access
EGU
Discussions

grassland area, and the shaded slope is also larger than the sunny slope (Fig.7).

According to the EMMA, precipitation and ground ice accounted for approximately 94% and 6% of soil water in the TRHR, respectively, during the end ablation period. All ground ice in soils below 4000 m at this time of year is ablated away, and all soil water is recharged by precipitation, with a small amount of ground ice water recharge occurring in the higher altitude areas. There is only a small amount of recharge from ground ice meltwater on shady slopes, which is still higher in meadow areas than in grassland areas (Fig.7).

4. Discussion

4.1 Influencing factors on soil water sources in different ablation periods

Various factors influence soil water sources, including temperature, precipitation, vegetation, evapotranspiration, and the freeze-thaw cycle. As mentioned above, soil water is mainly recharged by precipitation and ground ice meltwater, whereas the amount of ground ice is challenging to observe, so it is reflected by high or low ground temperature. As supplemental Fig.1 shows, spatial correlations of soil moisture with air and ground temperatures were analyzed during the sampling period. Interestingly, there was a positive correlation in the early ablation period because the active layer of permafrost is in the melting process. The higher

https://doi.org/10.5194/hess-2023-240
Preprint. Discussion started: 16 October 2023

Hydrology and Earth System Sciences
Open Access
EGU
Discussions

the ground temperature, the faster the ground ice melts, causing an increase in soil water, especially at lower altitudes. The liquid water produced by ground ice melting and the snow meltwater on the surface would move down to the upper limit of permafrost, and the precipitation will also move downward when the active layer completely melted, which would increase the soil water in the active layer (Jiao et al., 2014). Liquid soil water increased in the cold months under the increasing soil temperature and enhancing ground ice melting, while changes in the warm months were the results of competition between positive precipitation and adverse soil temperature effects in permafrost regions (Lan et al., 2015). The active permafrost layer melted slowly at higher altitude regions, and ~~the higher the ground temperature, the more evaporation occurred~~, causing a decrease in soil water. Wen et al. (2020) also indicated that temperature increases reduced the shallow soil water in cold regions. In the heavy ablation period, soil water exhibits a clear negative correlation with ground temperatures, with the end of thawing the active permafrost layer and the weakening effect of permafrost ground ice on soil water, and the higher the temperature, the stronger the evaporation and lower the soil water. Most regions display a clear positive correlation in September, with only a few lower altitude areas showing a negative correlation. Two reasons can account for it: (1) the top layer of soil at higher altitudes starts to freeze at night and thaws during the day, thus increasing soil water; (2) soil water at

https://doi.org/10.5194/hess-2023-240
Preprint. Discussion started: 16 October 2023

lower altitudes is affected by evaporation and decreases again. These facts also indicate that changes in freeze-thaw processes are an important influence on the evolution of soil water. During the thawing phase of the active permafrost layer, the increase in precipitation or soil water led to an increase in the thawing rate of frozen soil, accompanied by an increase in water infiltration as the frozen soil continued to thaw, leading to an increase in deep soil water and a decrease in surface soil water (Ma et al., 2021). Under freeze-thaw cycles, the adequate soil water in the root layers of different alpine meadows was ranked as follows: non-degraded meadow > moderately-degraded meadow > seriously degraded meadow (Lv et al., 2022). Xue et al. (2017) found that permafrost degradation significantly reduced soil water by 4.5–6.1% at a depth of 0–100 cm and increased the annual mean surface soil temperature by 0.8 °C in the source region of the Yangtze River.

Precipitation infiltration is considered the primary source of soil water in the active permafrost layer during the freeze-thaw action, which is considered a major factor and imposes limitations (Cao et al.,2018). In June, the spatial variation of soil water and precipitation in most regions, especially at high altitudes, shows a negative correlation; while only a few low-altitude regions show a positive correlation (supplemental Fig.2). Two reasons can account for it: 1) on the one hand, this indicates that precipitation in high altitude regions is mainly in the form of snowfall,

https://doi.org/10.5194/hess-2023-240
Preprint. Discussion started: 16 October 2023

which is difficult to recharge soil water directly, and the active permafrost layer melts slowly, and there is also the phenomenon of alternating between melting and freezing. So the more the precipitation there is, the less the soil water changes; 2) on the other hand, all the permafrost in low altitude regions melts during the season, and soil water is mainly recharged by precipitation, and the more precipitation, the higher the soil water. The correlation between soil water and precipitation is low during the warm season in permafrost areas and high in seasonal frozen areas because permafrost may help maintain soil water stability. In contrast, the permafrost degradation would reduce the regulating capacity of soil water, affecting the Tibetan Plateau ecosystem and hydrological cycle (Wu et al., 2021).

Soil water changes in August exhibit a significant negative correlation with precipitation. During this period, the active layer of permafrost melted. However, the source of soil water was mainly precipitation. More precipitation results in a higher quantity of soil water (supplemental Fig.2). Most areas show a positive correlation in September. Only a few high-altitude areas display a negative correlation; due to the temperature drop, precipitation in high-altitude areas is mainly snowfall, which has less effect on the recharge of soil water, while the lower altitude areas still show a positive correlation with rainfall, which directly recharges soil water. Deng et al. (2020) also indicated that soil water

https://doi.org/10.5194/hess-2023-240
Preprint. Discussion started: 16 October 2023

Hydrology and Earth System Sciences
Open Access
EGU
Discussions

increased with precipitation in most regions of TRHR. Based on the observation in TRHR, the soil water at 10 cm, 20 cm, and 30 cm increased by 0.47% /mm, 0.46% /mm, and 0.41% /mm, when the precipitation increased by 1 mm, while the soil water at 10 cm, 20 cm and 30 cm decreased by 3.8%/d, 3.3% /d and 2.3% /d when the number of days without precipitation increased by 1d, respectively (Li et al., 2022). The average soil water during 2003–2020 was 20%, increasing at a rate of 0.5%/10a, and its changes were influenced by precipitation and temperature in TRHR (Chen et al., 2021). In addition, the effect of snow cover on the soil water thawing up was greater than that of freezing, and the effect on shallow swamp soils was greater than that of shallow meadow soils (Chang et al., 2012).

Evapotranspiration is the reverse process of soil water recharge. Soil water, in general, shows a significant negative correlation with evapotranspiration in June, August, and September in TRHR, indicating that stronger evapotranspiration will result in less soil water (supplemental Fig.3). Based on observation under the simulated warming conditions in the Chengduo station in TRHR, the soil temperature increased by 2.50 ℃ and 1.36 ℃ at the soil depth of 0–15 cm and 15–30 cm, respectively, while the soil water decreased by 0.07% and 0.09% at the soil depth of 0–15 cm and 15–30 cm, respectively (Yao et al., 2019). Cao and Jin (2021) also concluded that soil water is negatively correlated with air temperature and

https://doi.org/10.5194/hess-2023-240
Preprint. Discussion started: 16 October 2023

positively correlated with precipitation.

4.2 Soil water sources and implications for vegetation restoration

As the limiting factor determining ecosystem stability in cold regions, there may be complex feedback relationships between vegetation and soil water. This is of great significance for improving the understanding of the hydrological process, soil and water conservation, and water resource utilization. As supplemental Fig.4 shows, the correlation between soil water and vegetation index in June is positive, and ~~the higher the altitude, the more significant the correlation~~. On the one hand, the vegetation has just resumed growth during this period, and the growth is slow with the relatively weak evapotranspiration, and because the soil is dry after a freezing period, the vegetation has a higher capacity to hold water; on the other hand, the active permafrost layer is still in the melting process, and the melting of ground ice increases the soil water accompanied by the continuous vegetation growth. In the early stage of vegetation growth, the upper soil layer has a high water-holding capacity, and the infiltration rate of precipitation was slow through the surface layer to the deeper layer of the soil, and there was a more uniform spatial distribution of soil water with the obvious water-holding function (Wang et al., 2003). Liu et al. (2021) also thought that the thawing of frozen soil increased the soil water in the root zone, regulated root respiration, and brought the vegetation into the growing season. Wei et al. (2022) also indicated that NDVI and surface

https://doi.org/10.5194/hess-2023-240
Preprint. Discussion started: 16 October 2023

soil water were positively correlated in the Loess Plateau with a more significant mutual feedback relationship.

Soil water displayed a negative correlation with vegetation index in most areas in August, reflecting better vegetation growth and stronger evapotranspiration, and lower soil water, as the active permafrost layer had all melted by that time of year. Vegetation was in an active growth phase. It showed a negative correlation with the vegetation index at most lower elevation areas in September, reflecting better vegetation growth, stronger evapotranspiration, and lower soil water; some higher elevations showed a positive correlation, reflecting the effects of the freeze-thaw cycle.

Soil water is, therefore, the basis of vegetation. The vegetation indices were closely associated with soil water, which played a key role in the active layer thickness-vegetation relationship, especially at depths of 30–40 cm in the northeastern Qinghai-Tibet Plateau (Jin et al., 2020). Thus, precipitation and vegetation were the main factors that caused soil moisture variation in summer and autumn, while the soil freeze-thaw cycle was the main contributing factor in spring (Ma et al., 2021). Based on the observation in the permafrost region, the mean surface soil water in the alpine meadow was higher than that in the alpine steppe, while soil water variability in the cold alpine steppe was larger than that in the alpine meadow, which decreased with depths (Yang et al., 2011). The soil water has reduced rapidly after the vegetation degeneration, especially in the soil depth of 0~30 cm, and so climate warming and permafrost degradation tend to decrease topsoil water in Tibetan Plateau (Wang et al., 2012). The soil water in the alpine steppe and temperate steppe were mainly affected by air temperature, and the influence factors for alpine meadow and shrub were precipitation and NDVI (Zhang et al., 2022). The effect of different vegetation types on the surface soil water varied widely, and the higher the vegetation cover, the greater increase in soil water (Ma, 2016). The surface soil water appeared to be significantly reduced with vegetation degradation. The more serious the degradation, the more the water loss (up to 38.6%) (Wang et al., 2010). In Qilian Mountains, the water loss has a clear positive relationship with soil water and a negative relationship with soil temperature for shrubland, grassland, and spruce forest (Hu et al., 2019). Lu et al. (2020) also thought community cover was sensitive to surface soil water and increased as a function of soil water from 1.1%–10.0% and gradually tended to saturate. There was a significant positive correlation between summer NPP and soil water in the watershed, but their interactions manifested spatial heterogeneity (Yue et al., 2021). Thus, the high soil water could support more plants with varied vegetation types (Jiao et al., 2020).

As mentioned above, the variability of soil water has further increased under warming, becoming the most critical factor affecting vegetation growth, especially as soil water loss will further exacerbate vegetation

https://doi.org/10.5194/hess-2023-240
Preprint. Discussion started: 16 October 2023

degradation and pose a great threat to the ecological security in the "Chinese water tower." Yue et al. (2022) also found that, under future climate change, only timely supplementing soil water could promote net primary productivity growth, improve vegetation productivity, and effectively restore and protect the ecological environment. Therefore, active measures should be taken in the following four aspects:

(1) Relying on ground-based meteorological observation stations, hydrological stations, and field observation stations, combined with remote sensing monitoring, to build a real-time observation network for soil water variation to provide data support for the formulation of scientific and reasonable water-soil conservation and vegetation restoration measures.

(2) In-depth research on the influence mechanism of soil water on vegetation growth, construction of vegetation growth model based on soil water and vegetation carrying capacity, the establishment of the soil water-vegetation change-vegetation restoration early warning platform, real-time early warning of vegetation degradation, and provision of the scientific basis for the restoration of degraded vegetation.

(3) The melting of the active permafrost layer and the change of soil water show seasonality, so the most suitable time for vegetation restoration should also be determined scientifically. In lower altitude regions, vegetation enters the growing season in June, and the restoration work should be implemented from the end of May to promote seed germination.

https://doi.org/10.5194/hess-2023-240
Preprint. Discussion started: 16 October 2023

Hydrology and Earth System Sciences Discussions
Open Access

In higher altitude regions, vegetation enters the growing season around the end of June, and in order to improve the survival rate of vegetation, rapid seed germination and breeding techniques should be developed. Mature seedlings should be directly transplanted to make full use of the short growing season to improve the effectiveness of vegetation restoration.

(4) There are significant differences in soil water and its environmental effects in grasslands, and restoration measures should be taken according to the different degradation degrees. The integrated pattern of winter rodent eradication + growing season grazing ban + fertilizer application technology is for the lightly degraded grasslands, which can significantly improve the vegetation cover and height of grasses and maintain a stable increase in soil water. The integrated pattern of winter rodent control + growing season grazing ban + fertilizer application + no-till replanting is for the moderately degraded grassland, which not only significantly increases the cover, height, amount of good forage and above-ground vegetation of grassland but also promotes the water-holding capacity. The integrated pattern of winter rodent eradication + growing season grazing ban + fertilizer application + re-vegetation technology is used in heavily degraded grasslands to restore vegetation and to ensure that soil water is stable enough to support vegetation growth.

(5) For areas of severe vegetation degradation, the focus is on the adequate compensation of precipitation in time and space. Changing the

https://doi.org/10.5194/hess-2023-240
Preprint. Discussion started: 16 October 2023

micro-topography to collect rainwater in the form of runoff or artificially produced flow, including fish-scale pit and horizontal ditch technologies, to achieve the objectives of water storage and moisture conservation, increase the survival rate of vegetation and improve ecological water use.

5. Conclusions

Based on 2600 samples of soil and surface water collected in the Three-River Headwater Region, the results indicated that δ18O and δD are relatively higher in June, then relatively negative in August, and then higher in September, while it exhibits an opposite trend for d-excess. The LEL and the relationship between soil water and surface waters in different ablation periods can confirm this. The intersection between the LWML and the LEL is considered to be the isotopic value of the initial water body that recharges the soil water, and the corresponding $\delta^{18}O$ and $\delta^{2}H$ are -17.63‰ and -127.61‰, -18.81‰ and -136.94‰, -23.04‰ and -170.36‰ during the early, heavy and end ablation period in the TRRH, respectively. These are close to the mean monthly precipitation values. Precipitation, ground ice, and snow meltwater accounted for approximately 72%, 20%, and 8% of soil water during the early ablation period, respectively, and it is with no snow meltwater recharge below 4000 m due to snow melting depletion. In the heavy ablation period, precipitation and ground ice contributed to 90% and 10% of soil water, respectively. The precipitation

https://doi.org/10.5194/hess-2023-240
Preprint. Discussion started: 16 October 2023

Hydrology and Earth System Sciences Discussions
Open Access
EGU

recharge decreases with increasing altitude, while ground ice gradually increases. According to the EMMA, it accounted for about 94% and 6% of soil water from precipitation and ground ice, respectively, during the end ablation period, and the small amount of recharge of ground ice mainly occurred in the area above 4000 m.

In the early ablation period, the higher temperature, the faster the ground ice melts, causing an increase in soil water, especially at lower altitudes. With higher temperature, more is the evaporation and lower is the soil water in the heavy ablation period. Most regions display a clear positive correlation in September owing to the freeze-thaw cycle. In June, soil water and precipitation show a negative correlation because there is mostly snowfall in high-altitude regions, whereas more the precipitation, the higher the soil water in August and September. However, heavy evapotranspiration will result in less soil water. It positively correlates with vegetation in June owing to the melting permafrost active layer, but the better vegetation growth, the lower soil water in August and September. However, soil water loss will further exacerbate vegetation degradation under warming and pose a significant threat to the ecological security of the "Chinese water tower." So, it is urgent to build the real-time soil water observation network, construct the soil water-vegetation change-vegetation restoration early warning platform, determine the most suitable time for vegetation restoration, and apply the different soil water

https://doi.org/10.5194/hess-2023-240
Preprint. Discussion started: 16 October 2023

Hydrology and Earth System Sciences
Discussions

conservation and vegetation recovery patterns.

Code/Data availability

The raw/processed data required to reproduce these findings cannot be shared at this time as the data also forms part of an ongoing study. We will not share our data until all relevant results are completed.

Author Contributions

Zongxing Li led the write-up of the manuscript with significant contribution. Zongxing Li developed the research and designed the experiments. Juan Gui and Baijuan Zhang collected the water samples and analysed the data. All authors discussed the results and contributed to the preparation of the manuscript.

Competing interests

This manuscript has not been published or presented elsewhere in part or in entirety and is not under consideration by another journal. We have read and understood your journal's policies, and we believe that neither the manuscript nor the study violates any of these. There are no conflicts of interest to declare.

Acknowledges

This study was supported by National Nature Science Foundation of and China(42077187), the Second Tibetan Plateau Scientific Expedition and Research Program (STEP, Grant No. 2019QZKK0405), the National Key Research and Development Program of China (Grant No. 2020YFA0607700), the "Western Light"-Key Laboratory Cooperative

Research Cross-Team Project of Chinese Academy of Sciences. We greatly appreciate suggestions from anonymous referees for the improvement of our paper. Thanks also to the editorial staff.

https://doi.org/10.5194/hess-2023-240
Preprint. Discussion started: 16 October 2023

Reference

Alexander Chumbaev. Hydrothermal regime of the urban soils in the cold period of the hydrological year of Western Siberia (Russia). International Journal of Biometeorology. 2021, 65: 1741-1750.

Beyer M, Hamutoko J T, Wanke H, Gaj M, Koeniger P. Examination of deep root water uptake using anomalies of soil water stable isotopes, depth-controlled isotopic labeling and mixing models. Journal of Hydrology, 2018, 566: 122–136.

Cao R, X M Jin. Distribution Characteristics of Soil Moisture in the Three Rivers Headwaters Region, China. Journal of Environmental Informatics Letters, 2021, 6(1): 55-65.

Cao W, Sheng Y, Wu JC, . Spatial variability and its main controlling factors of the permafrost soilmoisture on the northern-slope of Bayan Har Mountains in Qinghai-Tibet Plateau. Journal of Mountain Science, 2017, 14(12): 2406-2419.

Cao Wei, Sheng Yu, Wu Jichun, Wang Shengting, Ma Shuai. Seasonal variation of soil hydrological processes of active layer in source region of the Yellow River. Advances in Water Science, 2018, 29(1): 1-10.

Chang Juan, Wang Genxu, Gao Yongyong, Wang Yibo. Impacts of snow cover change on soil water-heat processes of swamp and meadow in Permafrost Region, Qinghai-Tibetan Plateau [J]. Acta Ecologica

https://doi.org/10.5194/hess-2023-240
Preprint. Discussion started: 16 October 2023

Hydrology and Earth System Sciences Discussions

Sinica, 2012, 32 (23): 7289-7301

Chen Guoqian, Zhu Cunxiong, Li Suyun, Zhou Bingrong, Li Fu, Cao Xiaoyun, Zhou Huakun. Remote sensing model constructions and spatial-temporal changes of soil moisture in the three-revier Headwaters Region. Acta Agrestia Sinica, 2021, 29: 199-207.

Chen Guoqian, Zhu Cunxiong, Li Suyun,Zhou Bingrong, Li Fu, Cao Xiaoyun, Zhou Huakun. Remote sensing model constructtions and spatial-temporal changes of soil moisture in the Three-river Headwaters Region. Remote Sensing of Environment, 2020, 247: 111727

Chen Yingying, Kun Yang, Juan Qin, Long Zhao, Wen Tang, Meng Han. Evaluation of AMSR-E retrievals and GLDAS simulations against observations of a soil moisture network on the central Tibetan Plateau. Journal of Rophysical Research , 2013, 118: 4466–4475.

Ma Chunfeng, Li Xin, Wei Long, Wang Weizhen. Multi-Scale Validation of SMAP Soil Moisture Products over Cold and Arid Regions in Northwestern China Using Distributed Ground Observation Data. Remote Sens. 2017, 327(09): 1-14.

Cosh M H, Jackson T J, Bindlish R, Prueger J H. Watershed scale temporal and spatial stability of soil moisture and its role in validating satellite estimates. Remote Sens. Environ, 2004, 92: 427–435.

Cuo Lan, Y Zhang, T J Bohn, L Zhao, J Li, Q Liu, B Zhou. Frozen soildegradation and its effects on surface hydrology in the northern Tibetan Plateau. Journal of Geophysical Research: Atmospheres, 2015, 120: 8276–8298.

D Liu , G Wang, R Mei, Z Yu, M Yu. Impact of initial soil moisture anomalies on climate mean and extremes over Asia. Journal of Rophysical Research, 2014, 119: 529-545

Di Ma, Siqiong Luo, Donglin Guo, Shihua Lyu, Xianhong Meng, Boli Chen, Lihui Luo. Simulated effect of soil freeze-thaw process on surface hydrologic and thermal fluxes in frozen ground region of the Northern Hemisphere[J]. Sciences in Cold and Arid Regions, 2021, 13(01): 18-29.

Dongxia Yue, Yanyan Zhou, Jianjun Guo, Zengzu Chao, Xiaojuan Guo. Relationship between net primary productivity and soil water content in the Shule River Basin. Catena, 2022, 208: 105770.

Gaj M, Beyer M, Koeniger P, Wanke H, Hamutoko J, Himmelsbach T. In situ unsaturated zone water stable isotope (^{2}H and ^{18}O) measurements in semi-arid environments: A soil water balance. Hydrology and Earth System Sciences, 2016, 20(2): 715–731.

Gao B, Yang D, Qin Y, Wang Y, Li H, Zhang Y , Zhang T. Change in frozen soils and its effect on regional hydrology in the upper Heihe Basin, the Northeast Qinghai-Tibetan plateau. Cryosphere Discuss, 2017, 289: 1–55.

Geris J, Tetzlaff D, McDonnell J J, Soulsby C. Spatial and temporal patterns of soil water storage and vegetation water use in humid Northern catchments. Science of the Total Environment, 2017, 595: 486–493.

Guimin Liu, Xiaoli Wu, Lin Zhao, Tonghua Wu, Guojie Hu, Ren Li, Yongping Qiao, Xiaodong Wu. Soil water content in permafrost regions exhibited smaller interannual changes than non-permafrost regions during 1986–2016 on the Qinghai-Tibetan Plateau. Catena, 2021, 207: 1056682.

Guo L, Zhu B, Jin H, Zhang Y, Min Y, He Y, Shi H. Spatial-Temporal Variation Characteristics and Influencing Factors of Soil Moisture in the Yellow River Basin Using ESA CCI SM Products. Atmosphere, 2022, 13: 962.

Huang Qian, Ding Mingjun, Chen Liwen, Xie Kun. variation of moisture in surface soil of alpine meadow with different degradation degrees in the Three-river sources region. Journal of Soil and Water Conservation, 2022, 36(1): 189-195.

Jia Li, Zuhao Zhou, Hao Wang, Jiajia Liu, Yangwen Jia, Peng Hu, Chong-Yu Xu. Development of WEP-COR model to simulate land surface water and energy budgets in a cold region. Hydrology Research, 2019, 50(1): 99-116.

Jian Hu, Da Lü, Feixiang Sun, Yihe Lü, Youjun Chen, Qingping Zhou. Soil

Hydrothermal Characteristics among Three Typical Vegetation Types: An Eco-Hydrological Analysis in the Qilian Mountains, China. Water, 2019, 11: 1277

Jiao Yongliang, Li Ren, Zhao Lin, Wu Tonghua, Xiao Yao, Hu Guojie, Qiao Yongping. Processes of soil thawing-freezing and features of soil moisture migration in the permafrost active layer[J]. Journal of Glaciology and Geocryology, 2014, 36 (02): 237-247.

Lei Jiao, Wenming An, Zongshan Li, Guangyao Gaoc, Cong Wang. Regional variation in soil water and vegetation characteristics in the Chinese Loess Plateau. Ecological Indicators, 2022, 115: 106399.

Li Fan, Yan Liangdong, Zhao Mengfan, Zhang Juan. Effect of precipitation in growing season on soil moisture in the Sanjiangyuan region. Journal of Arid Land Resources and Environment, 2022, 36(6): 121-128.

Li Fan, Yan Liangdong, Zhou Mengfan, Zhang Juan. Effect of precipitation in growing season on soil moisture in the Sanjiangyuan region. Journal of Arid Land Resources and Environment, 2022, 33(6): 121-128.

Li Z, Ma J, Song L, Juan Gui, Jian Xue, Baijuan Zhang, Wende Gao, Zongxing Li. Investigation of soil water hydrological process in the permafrost active layer using stable isotopes. Hydrological Processes. 2020, 34: 2810–2822.

https://doi.org/10.5194/hess-2023-240
Preprint. Discussion started: 16 October 2023

Liu Zhenhai, Wang Shaoqiang, Chen Bin. Spatial and temporal variations of frozen ground and its vegetation response in the eastern segment of China-Mongolia-Russia economic corridor from 2000 to 2015. Acta Geographica Sinica, 2021, 76(5): 1231-1244.

Longwei Xiang, Hansheng Wang, Holger Steffen, Patrick Wu , Lulu Jia ,Liming Jiang , Qiang Shen. Groundwater storage changes in the Tibetan Plateau and adjacent areas revealed from GRACE satellite gravity data. Earth and Planetary Science Letters, 2016, 449: 228–239.

Lu Fengshuai, Ade LuJi, Cheng Yunxiang, *et al*. Relationship between soil moisture and vegetation coverin Qilian Mountain alpinesteppe. Acta Prataculturae Sinica, 2020, 29(11): 23-32.

Ma Zhiang. Study on Temporal-spatial Pattern and Influencing Factors of Soil Moisture Based on Remote Sensing in the Source Region of Yellow River. Master's Thesis, Gansu Agricultural University, 2016.

Marchionni V, Fatichi S, Tapper N, Walker J, Manoli J, Daly E. Assessing vegetation response to irrigation strategies and soil properties in an urban reserve in southeast Australia. Landscape Urban Plann. 2021 215: 104-198.

Martínez García G, Pachepsky Y A, Vereecken, H. Effect of soil hydraulic properties on the relationship between the spatial mean and variability of soil moisture. J. Hydrol, 2014, 516: 154–160.

Masato Shinoda, Banzragch Nandintsetseg. Soil moisture and vegetation memories in a cold, arid climate. Global and Planetary Change, 2020, 79: 110-117.

Mingshan Deng, Xianhong Meng, Zhaoguo Li,mYaqiong Lyv, Huajin Lei1, Lin Zhao, Shengnan Zhao, Jun Ge, Hui Jing. Responses of soil moisture to regional climate change over the Three Rivers Source Region on the Tibetan Plateau. International Journal of Climatol. 2020, 40:2403-2417.

Mingxia Lv, Yibo Wang, Zeyong Gao. The change process of soil hydrological properties in the permafrost active layer of the Qinghai–Tibet Plateau. Catena, 2022, 210: 05938.

Qi W, Feng L, Liu J, Yang H. Snow as an important natural reservoir for runoff and soil moisture in Northeast China. Journal of Geophysical Research: Atmospheres, 2022, 25: 33-86.

R Cao, X M Jin. Distribution Characteristics of Soil Moisture in the Three Rivers Headwaters Region, China. Journal of Environmental Informatics Letters, 2021, 6(1): 55-65.

Sazib N, Bolten J, Mladenova I. Exploring spatiotemporal relations between soil moisture, precipitation, and streamflow for a large set of watersheds using google earth engine. Water, 2020, 12 (5): 13-71.

Song Lingling, Li Zongjie, Tian Qing, Wang Liefu, He Jing, Yuan Ruifeng, Gui Juan, Zhang Baijuan, Lv Yuemin. Variation and relationship between soil moisture and environmental factors in the source region

https://doi.org/10.5194/hess-2023-240
Preprint. Discussion started: 16 October 2023

Hydrology and Earth System Sciences Discussions
Open Access

of the Yangtze River from 2005 to 2016. Sciences in Cold and Arid Regions, 2019, 11(3): 184−193.

Spennemann P C, Salvia M, Ruscica R C, Sorensson A A, Grings F, Karszenbaum H. Land-atmosphere interaction patterns in southeastern South America using satellite products and climate models. International Journal of Applied Earth Observation and Geoinformation, 2018, 64: 96-103.

Sprenger M, Tetzlaff D, Soulsby C. Soil water stable isotopes reveal evaporation dynamics at the soil–plant–atmosphere interface of the critical zone. Hydrology and Earth System Sciences, 2017, 21: 3839–3858.

Tan H, Liu Z, Rao W, Wei H, Zhang Y, Jin B. Stable isotopesof soil water: Implications for soil water and shallow groundwater recharge in hill and gully regions of the loess plateau, China. Agriculture, Ecosystems & Environment, 2017, 243: 1–9.

W Wagner, K Scipal, C Pathe, D Gerten, W Lucht, B Rudolf. Evaluation of the agreement between the first global remotely sensed soil moisture data with model and precipitation data. Journal of Geophysical Research, 2003, 108(D19): 46-11

Wang Genxu, Shen Yongping, Qin Ju, Wang Junde. Study on the Influence of Vegetation Change on Soil Moisture Cycle in Alpine Meadow. Journal of Glaciology and Geocryology, 2003, 25(6): 329-337.

https://doi.org/10.5194/hess-2023-240
Preprint. Discussion started: 16 October 2023

Wang Yibo, Niu Fujun, Wen Jing, Wu Qingbai, Zhang Wei. Study of the Soil Hydrological Process in the Source Regions of the Yangtze River, China. Advanced Materials Research,2012, 518-523: 4266-4272.

Wang Yibo, Niu Fujun, Wen Jing, Wu Qingbai, Zhang Wei. Study of the Soil hydrological Process in the Source Regions of the Yangtze River, China. Advanced Materials Research Vols, 2012, 518-523: 4266-4272.

Wang Yibo, Wang Genxu, Wu Qingbai, Niu Fujjun, Chen Huiyan. The impact of vegetation degeneration of Hydrology features of alpine soil. Journal of Glaciology and Geocryology, 2010, 32(5): 989-998.

Wen Jing, Qin Ruimin, Zhang Shixiong, Yang Xiaoyan, Xu Manhou. Effects of long-term warming on the aboveground biomass and species diversity in an alpine meadow on the Qinghai-Tibetan Plateau of China. Journal of Arid Land, 2020, 12(2): 252–266.

Wu Xiaoli, Liu Guimin, Li Xinxing, Ji Genghao, Li Lisha, Mao Nan, Xu Haiyan, Wu Xiaodong. Variation of Soil Moisture and Its Relation with Precipitation of Permafrost and Seasonally Frozen Soil Regions on the Qinghai-Tibet Plateau. Journal of China Hydrology, 2021, 41(1): 73-79.

X J Guan1, C J Westbrook1 , C Spence. Shallow soil moisture-ground thaw interactions and controls-Part 1: Spatiotemporal patterns and correlations over a subarctic landscape. Hydrology and Earth System Sciences, 2020, 14(07): 1375–1386.

https://doi.org/10.5194/hess-2023-240
Preprint. Discussion started: 16 October 2023

Hydrology and Earth System Sciences Discussions

Xian Xue, Quangang You, Fei Peng, Siyang Dong, Hanchen Duan. Experimental warming aggravates degradation-induced topsoil drought in alpine meadows of the Qinghai-Tibetan Plateau. Land Degrad Develop, 2017, 28: 2343–2353.

Xiaoting Wei, Qiang Huang, Shengzhi Huang , Guoyong Leng , Yanping Qu, Mingjiang Deng, Zhiming Han, Jing Zhao, Dong Liu, Qingjun Bai. Assessing the feedback relationship between vegetation and soil moisture over the Loess Plateau, China. Ecological Indicators, 2022, 134: 108493.

Xiaoying Jin, Huijun Jin, Xiaodong Wu, Dongliang Luo , Sheng Yu, Xiaoying Li, Ruixia He, QingfengWang, Johannes M. H. Knops. Permafrost Degradation Leads to Biomass andSpecies Richness Decreases on the NortheasternQinghai-Tibet Plateau. Plants, 2020, 9(11):14-53.

Xue Xian, You Quangang, Peng Fei, Dong Siyang, Duan Hanchen. Experimental warming aggravates degradation-induced topsoil drought in alpine meadows of the qinghai–tibetan plateau. Land Degrad Develop, 2017, 28: 2343–2353.

Yao Shiting, Lu Guangxin, Li Xin, Dang Ning, Wang Yingcheng, Zhou Jie Dongzhu, Fu Gang, Wang Junbang, Zhou Huakun. Effects of simulated warming on soil moisture of alpine meadow at Chengduo of Yushu Prefecture, Qinghai province. Ecology and Environmental

Sciences, 2019, 28(11): 2176-2184.

Yue Dongxia, Mu Xinliang, Zhou Yanyan, Guo Xiaojuan, Wei Lemin, Guo Jianjun. Coupling relationship between net primary productivity and soil moisture content in the Shule River Basin. Journal of Lanzhou University (Natural Sciences), 2021, 57(4): 518-527.

Zhang Mengy, Ma Yujun, Xie Ting. Spatial distribution characteristics of soil moisture during growing season in Qinghai Lake Basin. Water Resources and Hydropower Engineering, 2022, 1-15

Zhang Z, Lv Q, Guo Z, Huang X, Hao R. Soil Water Movement of Mining Waste Rock and the Effect on Plant Growth in Arid, Cold Regions of Xinjiang, China. Water, 2021, 13(09):12-40.

Zhaoping Yang, Hua Ouyang, Xianzhou Zhang, Xingliang Xu, Caiping Zhou, Wenbin Yang. Spatial variability of soil moisture at typical alpine meadow and steppe sites in the Qinghai-Tibetan Plateau permafrost region. Environ Earth Sci , 2011, 63: 477–488.

Zhe Zhang, Yanping Li, Fei Chen, Michael Barlage, Zhenhua Li. Evaluation of convection-permitting WRF CONUS simulation on the relationship between soil moisture and heatwaves. Climate Dynamics, 2020, 55: 35-252.

https://doi.org/10.5194/hess-2023-240
Preprint. Discussion started: 16 October 2023

Tables

Table.1 The average values of stable isotopes and relationship between $\delta^{18}O$ and d-excess for soil waters in TRHR

	Relationship between $\delta^{18}O$ and d-excess/ R^2	average values for: $\delta^{18}O$, δ^2H and d-excess in June	average values for: $\delta^{18}O$, δ^2H and d-excess in August	average values for: $\delta^{18}O$, δ^2H and d-excess in Sepetember
All soil water samples	Y=-0.16x+3.87, R^2=0.0065	-12.00; -89.78; 6.30	-13.26; - 100.0; 8.58	-13.04; - 98.11; 6.24
0-20cm	Y=-0.43x+0.98, R^2=0.065	-11.91; -90.07; 5.18	-13.24; - 101.44; 8.87	-14.23; - 108.14; 5.71
20-40cm	Y=-0.4564x+0.7948, R^2=0.0392	-12.07; -90.74; 5.84	-12.96; - 99.01; 11.23	-12.42; - 92.72; 6.61
40-60cm	Y=-1.05x-7.33, R^2=0.1667	-12.38; -90.38; 8.68	-13.63; - 101.46; 5.67	-12.33; - 92.06; 6.55
60-80cm	Y=-0.32x+2.5781, R^2=0.0167	-11.36; -83.77; 7.09	-13.32; - 98.51; 4.17	-12.42; - 92.88; 6.45
Northern slope	Y=-1.1944x-7.3393,	-12.33; -90.61; 7.99	-13.07; - 98.34; 12.45	-12.05; - 91.64; 4.75
Eastern slope	R^2=0.1584	-11.96; -91.15; 4.54	-13.06; - 99.61; 6.04	-18.163; - 137.38; 7.93
Southern slope	Y=-0.7x-2.2479, R^2=0.0956	-11.31; -85.49; 5.028	-13.77; - 103.422; 6.16	-12.17; -89.9; 7.47
Western slope	Y=-0.4337x+0.8866, R^2=0.0543	-12.62; -93.63; 7.36	-12.92; - 96.89; 11.99	-12.2; -91.5; 6.15
Grassland	Y=-0.4921x-0.5722, R^2=0.0715	-10.39; -77.66; 5.45	-12.13; - 89.28; 27.06	-9.62; - 71.87; 5.13
Meadow	Y=-0.6067x+0.8133, R^2=0.0615	-12.15; -90.36; 6.87	-13.45; - 101.94; 5.25	-12.82; - 96.56; 6.02

https://doi.org/10.5194/hess-2023-240
Preprint. Discussion started: 16 October 2023

Hydrology and Earth System Sciences
Open Access
EGU
Discussions

Forest	Y=-1.4013x-12.706, R^2=0.2283	-13.6; -103.66; 5.1	-13.66; -103.16; 5.24	-15.82; -118.98; 7.60

Table.2 The LEL for soil waters in study region

	EL/ R^2 in June	EL/ R^2 in August	EL/ R^2 in September
2900-3500	$\delta^2H = 5.7\delta^{18}O - 21.18$ R^2=0.90	$\delta^2H = 6.8\delta^{18}O - 7.83$ R^2=0.95	**$\delta^2H = 7.43\delta^{18}O - 2.59$ R^2=0.98**
3500-4000	$\delta^2H = 7.58\delta^{18}O - 1.34$ R^2=0.83	$\delta^2H = 6.48\delta^{18}O - 16.54$ R^2=0.9	$\delta^2H = 7.67\delta^{18}O + 3.1$ R^2=0.97
4000-4500	$\delta^2H = 7.27\delta^{18}O - 3.46$ R^2=0.88	$\delta^2H = 6.5\delta^{18}O - 15.09$ R^2=0.93	$\delta^2H = 7.04\delta^{18}O - 6.8$ R^2=0.96
nibanshi4500-5100	$\delta^2H = 6.05\delta^{18}O - 12.4$ R^2=0.85	$\delta^2H = 6.69\delta^{18}O - 8.68$ R^2=0.93	$\delta^2H = 6.9\delta^{18}O - 6.6$ R^2=0.87
grassland	$\delta^2H = 6.4\delta^{18}O - 11.07$ R^2=0.83	$\delta^2H = 6.62\delta^{18}O - 9.07$ R^2=0.96	$\delta^2H = 6.44\delta^{18}O - 9.91$ R^2=0.92
meadow	$\delta^2H = 6.55\delta^{18}O - 10.67$ R^2=0.84	$\delta^2H = 6.4\delta^{18}O - 15.83$ R^2=0.90	$\delta^2H = 7.14\delta^{18}O - 5.05$ R^2=0.95
forest	$\delta^2H = 6.97\delta^{18}O - 8.9$$R^2$=0.73	$\delta^2H = 7.61\delta^{18}O + 0.85$$R^2$=0.97	$\delta^2H = 7.46\delta^{18}O - 0.97$$R^2$=0.97
Northern slope	$\delta^2H = 7.33\delta^{18}O - 0.22$ R^2=0.84	$\delta^2H = 6.8\delta^{18}O - 9.46$ R^2=0.91	$\delta^2H = 6.86\delta^{18}O - 8.95$ R^2=0.90
Eastern slope	$\delta^2H = 6.92\delta^{18}O - 8.38$ R^2=0.88	$\delta^2H = 6.33\delta^{18}O - 16.9$ R^2=0.89	$\delta^2H = 6.78\delta^{18}O - 14.253$ R^2=0.93
Southern slope	$\delta^2H = 6.44\delta^{18}O - 13.22$ R^2=0.81	$\delta^2H = 6.84\delta^{18}O - 9.28$ R^2=0.96	$\delta^2H = 6.8\delta^{18}O - 7.0$ R^2=0.93
Western slope	$\delta^2H = 6.14\delta^{18}O - 16.14$ R^2=0.91	$\delta^2H = 6.46\delta^{18}O - 13.4$ R^2=0.92	$\delta^2H = 7.33\delta^{18}O - 2.07$ R^2=0.98

https://doi.org/10.5194/hess-2023-240
Preprint. Discussion started: 16 October 2023

Hydrology and Earth System Sciences Discussions

Figures

Fig.1 The location of Three -River Headwater Region in ecological barriers of China(a); distribution map of permafrost and seasonal frozen soil (b), soil types (c) and vegetation types (d) in the study region

Fig.2 the work photo for sampling glacier snow meltwater(a), soil in grassland(b), soil in meadow (c), supre-permafrost water (d), river water (e), tributary water (f), vegetation (g) and soil in forests (h)

Fig.3 Distribution of sampling sites for soils and waters in June (a), August (b) and September (c)

Fig.4 Plot of δD versus $\delta^{18}O$ and LEL for soil water at different soil layers on June (a), August (b) and September (c)

Fig.5 Hydraulic connections between soil water and other waters for all samples (a), different altitudes (b) and vegetation (c) in June, all samples (d), different altitudes (e) and vegetation (f) in August, all samples (g), different altitudes (h) and vegetation (i) in September

Fig.6 Three end element diagram in June (a) and Two end element diagram in August (b) and September (c) using the mean values of $\delta^{18}O$ and d-excess for soil water

Fig.7 Concept map for contribution from precipitation, snow meltwater and ground ice to soil water in the whole study region, different altitudes and different vegetation in June (a), August (b) and September (c)

https://doi.org/10.5194/hess-2023-240
Preprint. Discussion started: 16 October 2023

Hydrology and Earth System Sciences
Discussions

Fig.8 Concept diagram for real-time monitoring network for soil water, soil water-vegetation change-vegetation restoration early warning platform and the different soil water conservation and vegetation restoration patterns in Three-River Headwater Region

https://doi.org/10.5194/hess-2023-240
Preprint. Discussion started: 16 October 2023

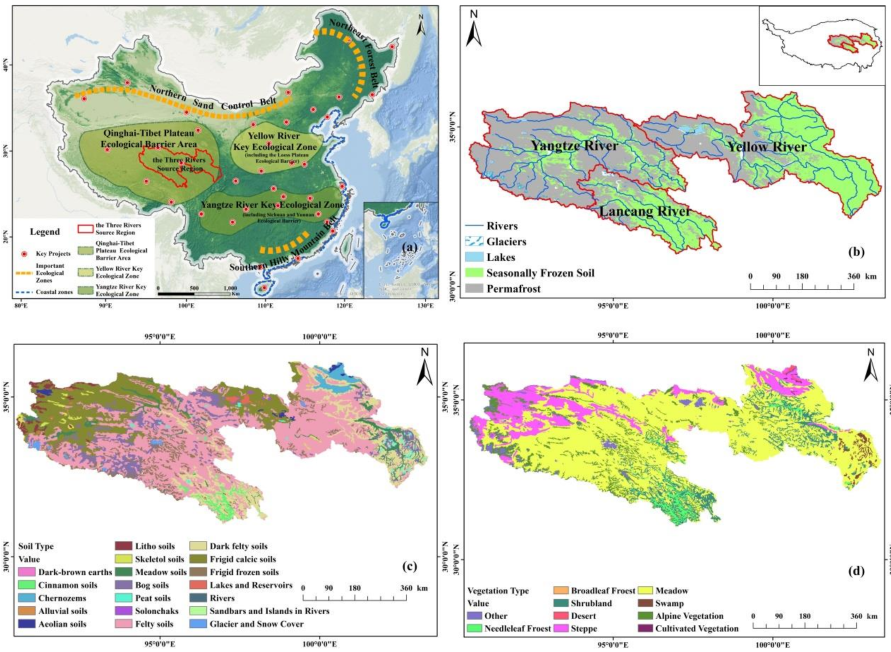

Fig.1

Fig.2

https://doi.org/10.5194/hess-2023-240
Preprint. Discussion started: 16 October 2023

Hydrology and Earth System Sciences
Discussions

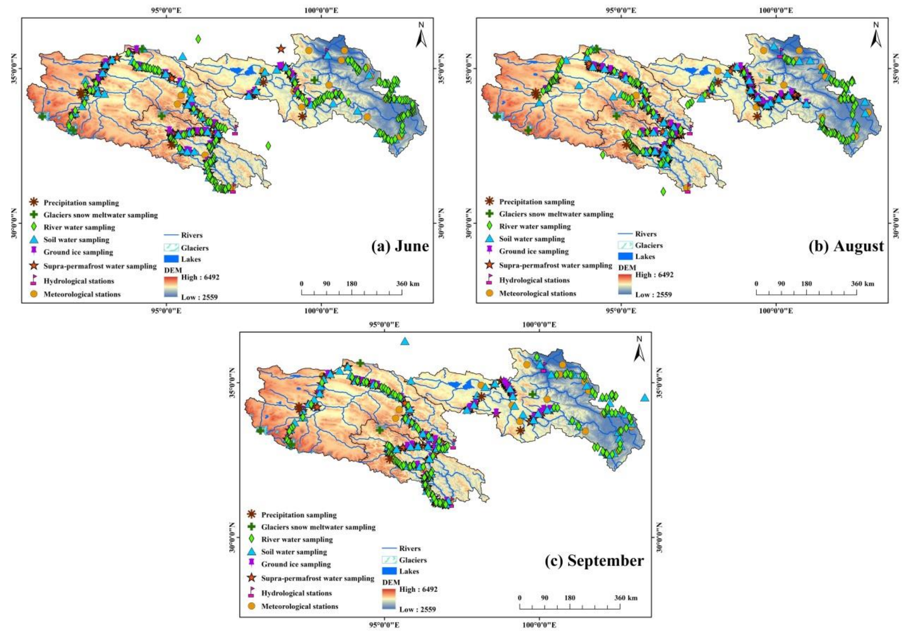

Fig.3

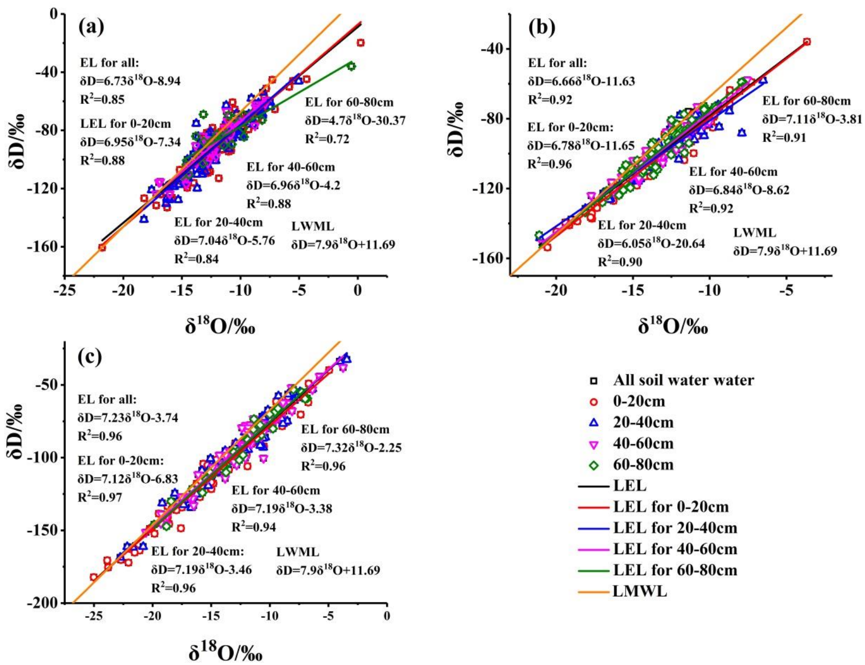

Fig.4

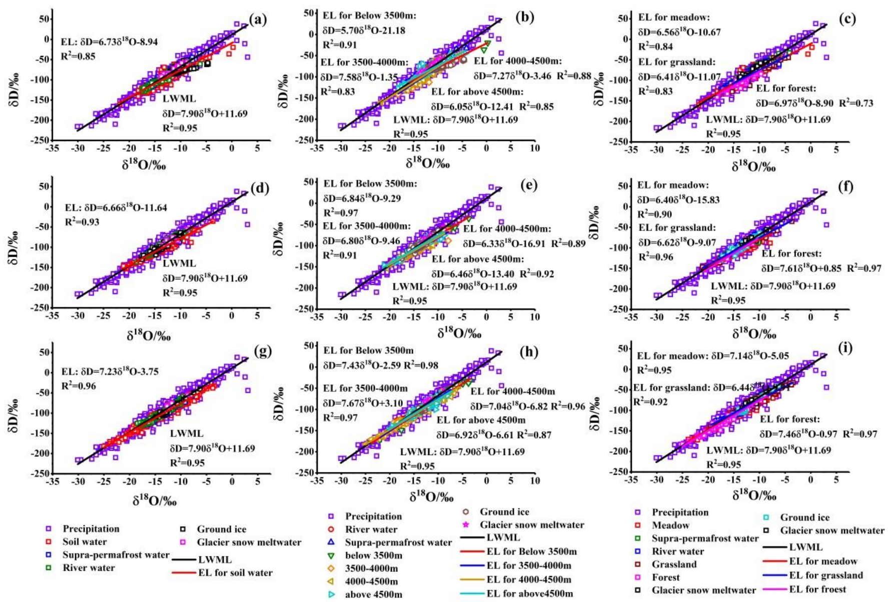
(a)
(b)
(c)
(d)
(e)
(f)
(g)
(h)
(i)
δD/‰
δ18O/‰
Precipitation
Soil water
Supra-permafrost water
River water
Ground ice
Glacier snow meltwater
LWML
EL for soil water
below 3500m
3500-4000m
4000-4500m
above 4500m
EL for Below 3500m
EL for 3500-4000m
EL for 4000-4500m
EL for above4500m
Meadow
Grassland
Forest
EL for meadow
EL for grassland
EL for froest

Fig.5

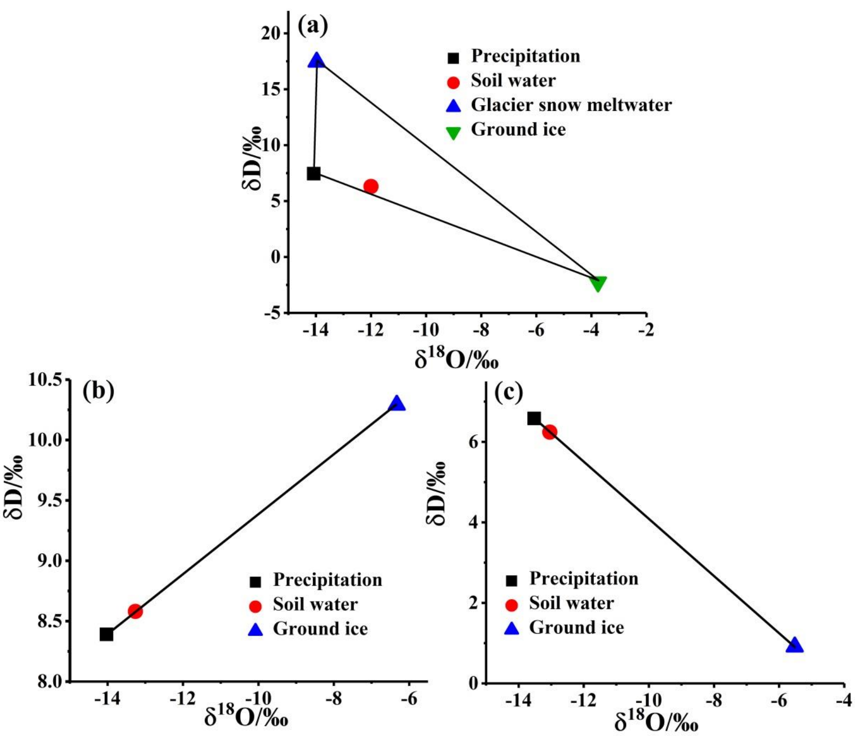
(a)
Precipitation
Soil water
Glacier snow meltwater
Ground ice
δD/‰
δ18O/‰
(b)
Precipitation
Soil water
Ground ice
δD/‰
δ18O/‰
(c)
Precipitation
Soil water
Ground ice
δD/‰
δ18O/‰

Fig.6

https://doi.org/10.5194/hess-2023-240
Preprint. Discussion started: 16 October 2023

Hydrology and Earth System Sciences
Open Access
Discussions

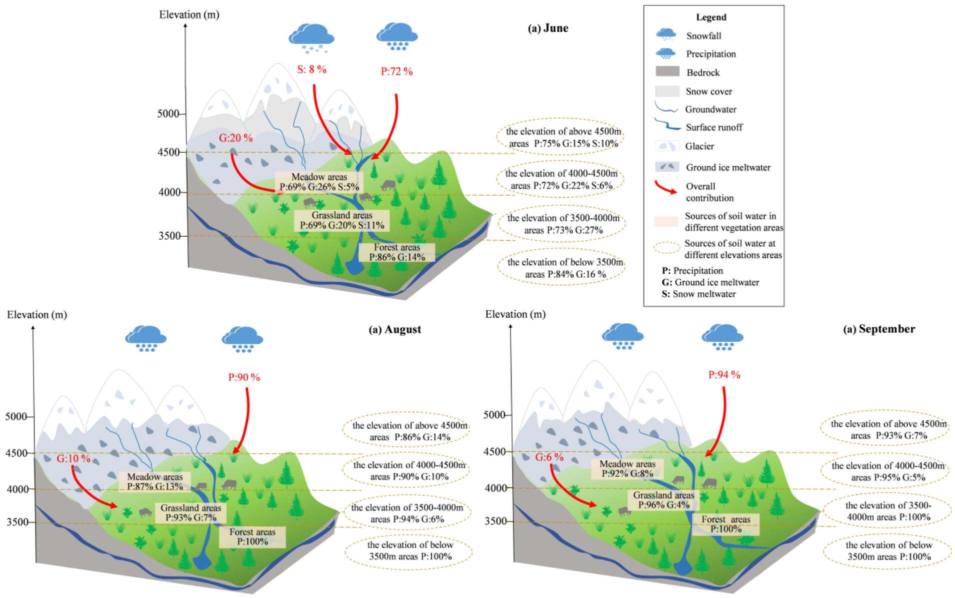

Fig.7

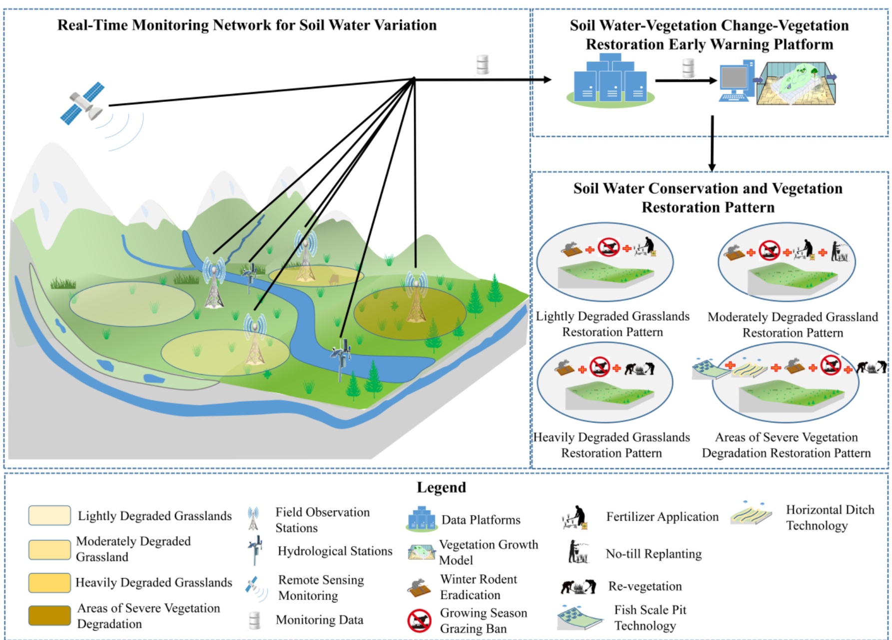

Fig.8